Circular Hydrogen Bond Networks on the Surface of β-Ribofuranose in Aqueous Solution

Teppei Suzuki* and Takayuki Sota

Integrative Bioscience and Biomedical Engineering, Graduate School of Science and Engineering, Waseda University, 3-4-1 Okubo, Shinjuku, Tokyo 169-8555, Japan

Received: January 7, 2005; In Final Form: March 29, 2005

This paper examines the hydration structure on the surface of β-ribofuranose in aqueous solution, using the ab initio molecular dynamics method. In particular, we focus on circular hydrogen bond networks involving two ribofuranose oxygens and three water molecules. In our simulations, the circular hydrogen bond networks near the ring oxygen of β-ribofuranose are found to be significantly influenced by the orientation of the hydroxymethyl group. The arrangements of hydrogen bonds observed in the circular hydrogen bond networks are both homodromic and antidromic. To explain these observations, we analyze the electronic properties of the first-hydration-shell water molecules and the OH groups of β-ribofuranose, using the centers of their maximally localized Wannier functions. The dipole moments of the proton-accepting first-hydration-shell water molecules in our well-defined circular hydrogen bond networks are found to increase by about 0.3 D compared with that of liquid water, indicating the relatively strong polarization effects created by the interactions between the OH groups of the solute and the surrounding water molecules. Our analysis also implies that circular H-bond networks cannot be fully explained from a simple geometrical point of view.

Introduction

Understanding how monosaccharides are hydrated is critical to understanding their conformations, such as the distributions of the rotamers, and their biological activities. However, the microscopic hydration mechanism of monosaccharides is still uncharacterized and poorly understood. Explanations for the hydration of monosaccharides date back to the view of Kabayama and Patterson,[1] in which the preference of the β anomer of glucopyranose over the α anomer in aqueous solution is explained by the structural compatibility between the β anomer and the icelike lattice of water. Computational studies[2−5] focused on water structuring around monosaccharides and arrived at no evidence for these kinds of icelike hydration structures, and one of them led to a somewhat contrasting idea, *anisotropic solvent structuring* depending on molecular topologies.[3] The other model[6] for the hydration of monosaccharides, which is similar to the Kabayama−Patterson one, is based on the assumption that an equatorial hydroxyl group might be better hydrated without causing the strain of an icelike lattice than an axial one. This model was later extended into related ones that regard the *dynamic hydration number*[7,8] or the number of equatorial hydroxyl groups[8] as a dynamical parameter for characterizing the hydration of monosaccharides. Other authors refined the earlier qualitative description[9] and emphasized the stereochemical aspects of hexose hydration, especially its correlation with the relative orientations of a particular pair of hydroxyl groups.[10] A rather different attempt to describe the interactions between sugar and water molecules was made by Saenger,[11] who introduced the concept of *circular hydrogen bonds.* This concept was derived by considering the results of X-ray and neutron diffraction experiments on the crystal structures of α-cyclodextrin (consisting of six α-glucose molecules) hexahydrate. However, the application of this concept was limited only to the cyclodextrin−water interaction,[11−13] to the best of our knowledge.

Many theoretical studies have been devoted to understanding the behavior of monosaccharides, especially that of glucopyranose. In addition to the gas-phase studies[14−30] and calculations of its crystalline structures,[31−33] there are many computational studies focusing on many properties of glucopyranose in aqueous solution, by quantum chemical methods including solvation models,[34−38] as well as several explicit water molecules[39−41] and by molecular dynamics (MD) simulations.[2−5,42−47] Moreover, recent computational studies suggest that surrounding water molecules are essential to computational studies of carbohydrates in aqueous solution, for example, in reproducing experimental rotamer distributions of carbohydrates[48] and the spectroscopic properties of glucose solution in a particular wavenumber region[41] and in determining the relative stabilities of glucopyranose conformers in aqueous solution.[47] Also, because of the relevance as building blocks of RNA, ribofuranose and its derivatives have also been studied.[49−68] In particular, many theoretical efforts using quantum chemical approaches have been devoted to the structural and conformational properties of furanoses, especially the relationships between puckering phase angle and their structural parameters.[49−57]

Despite all this, the hydration of β-ribofuranose remains poorly understood.[69] A better understanding of the hydration of β-ribofuranose is essential, for example, for understanding nucleic acids in aqueous solution. With this perspective, in this paper, we examine the hydrogen bond (H-bond) network structure on the surface of β-ribofuranose in aqueous solution, using Car−Parrinello molecular dynamics (CPMD) simulations.[70] Since ab initio MD simulation is still computationally demanding, the conformers are unavoidably limited; in the present work, we consider two hydroxymethyl rotamers of β-ribofuranose in the north[71] form. However, ab initio MD simulations allow us to investigate the local polarization effects

* Corresponding author. E-mail: teppei_suzuki@moegi.waseda.jp.

10.1021/jp050100x CCC: $30.25
Published on Web 06/04/2005

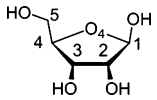

Figure 1. Atom labeling scheme of β-ribofuranose. Throughout the paper, the hydroxymethyl rotamers of β-ribofuranose are defined by the O4−C4−C5−O5 dihedral angle, which can be $\approx +60°$ (G^+ or *gt*), $-60°$ (G^- or *gg*), or 180° (T or *tg*).

created by the interactions between the OH groups of β-ribofuranose and surrounding water molecules, using the centers of their maximally localized Wannier functions. This kind of analysis could offer valuable insight into the hydration of β-ribofuranose.

This paper is organized as follows. After giving computational details of our simulations, we examine the average number of intermolecular H-bonds in the hydrated β-ribofuranose and the ribofuranose−oxygen−water−oxygen pair correlation functions. Next, we investigate the circular H-bond networks on the surface of β-ribofuranose. In particular, we report that the circular H-bond networks near the ring oxygen are fairly influenced by the orientation of the hydroxymethyl group. To explain our circular H-bond networks, we also examine the electronic properties of the OH groups of β-ribofuranose and the first-hydration-shell water molecules, using the centers of their maximally localized Wannier orbitals. Then, we draw the conclusions and some implications.

Simulation Models and Computational Details

The β-ribofuranose−water system was modeled in a cubic supercell of side 12.68 Å with periodic boundary conditions, containing 60 H_2O molecules and 1 β-ribofuranose molecule (corresponding to a 1 g/cm^3 density). In the present work, we considered two hydroxymethyl rotamers (G^+ and G^-). For the definition, see the caption of Figure 1) of β-ribofuranose in the north form. The mass of deuterium was not used for hydrogen. The electronic structure calculations were carried out in the framework of the Kohn−Sham formulation of density functional theory.[72] The gradient-corrected BLYP (Becke, Lee, Yang, and Parr) exchange-correlation functional[73] was used because it proved to be reasonably accurate in describing many properties of aqueous systems[74,75] as well as hydrated biological molecules.[76] The valence electronic wave functions were expanded in a plane wave basis set up to a kinetic energy cutoff of 70 Ry, and the valence-core interactions were treated by norm-conserving, separable dual-space Gaussian pseudopotentials by Goedecker, Teter, and Hutter,[77] which have analytic forms and give the optimal efficiency in numerical calculations when using plane waves as a basis set. Only the Γ point was used to sample the Brillouin zone. Our ab initio MD simulations were performed using cpmd code.[78] The Car−Parrinello equations of motion[79] were integrated using a time step of 0.0968 fs and a fictitious electronic mass of 400 au. Recently, Grossman et al.[80] performed the CPMD simulations of both liquid H_2O and D_2O under ambient conditions, using two different values for a fictitious mass: $\mu = 340$ and 760 au. According to their report, for pure liquid water, the use of relatively large fictitious masses ($\mu/M \geq {}^1/_3$, where M denotes an ionic mass, which is typically that of H or D) artificially softens the oxygen−oxygen pair correlation function of liquid water.[80] In the present work, the ratio of the fictitious mass to the ionic one is about 0.22, which is smaller than ${}^1/_3$. Kuo et al.[81] recently suggested that a fictitious mass of 400 au is small enough for microcanonical CPMD simulations of liquid H_2O under ambient conditions even for longer simulation runs (more than 10 ps). From these reports, for our particular systems, a fictitious mass of 400 au is considered to be small enough to avoid the artifact that might cause the broadness of our β-ribofuranose−oxygen−water−oxygen pair correlation functions. Our simulations consisted of an initial equilibration phase of 3 ps using the Nosé−Hoover chain thermostat method[82] to control the ionic temperature at about 300 K, followed by a microcanonical MD run of 6 ps, in which the average ionic temperatures of the simulations of the G^- and G^+ rotamers were 296 and 297 K, respectively.

Results and Discussion

Before analyzing the H-bond structures of β-ribofuranose, we confirmed by monitoring the trajectories that neither of the two simulations underwent the transition between the north and south regions; by checking the time series of the dihedral angles of the hydroxymethyl group for the two rotamers, we also found that neither of the two simulations underwent the reorientation of the hydroxymethyl group (the average dihedral angles of the hydroxymethyl group for G^- and G^+ were -68.5 ± 11.3 and $67.0 \pm 7.9°$, respectively). Additionally, we looked at the time series of the hydroxyl groups: The average O4−C1−O1−H1, C1−C2−O2−H2, C2−C3−O3−H3, and C4−C5−O5−H5 torsion angles in the microcanonical simulation of the G^+ rotamer were -68.0 ± 13.8, -35.2 ± 13.5, -51.2 ± 20.4, and $84.7 \pm 15.8°$, respectively. The average C2−C3−O3−H3 and C4−C5−O5−H5 torsion angles in the microcanonical simulation of the G^- rotamer were 84.0 ± 23.7 and $66.1 \pm 18.3°$, respectively. However, the O4−C1−O1−H1 torsion angle was highly scattered by intermolecular H-bonds with water molecules (the average value in the first 1 ps was $-124.3 \pm 17.6°$, whereas the one in the last 3 ps was $110.8 \pm 34.6°$). The C1−C2−O2−H2 torsion angle experienced a reorientation due to the formation of an intramolecular H-bond between H2 and O3, at 5.0−6.0 ps in the microcanonical run (the average value in the first 4 ps was $104.9 \pm 27.7°$, whereas the one in the last 1 ps was $12.5 \pm 23.6°$).

After we had checked out the conformations, we compared the average total number of intermolecular H-bonds in the hydrated β-ribofuranose and the one in the hydrated β-glucopyranose.[5] In our analysis, we used the criteria for the existence of an H-bond (O_D−H···O_A) of O_D−H ≤ 1.5 Å, H···O_A ≤ 2.4 Å, and $\angle O_DHO_A > 120°$, where O_D and O_A are proton-donor and proton-acceptor oxygens, respectively. The average numbers of intermolecular H-bonds for G^- and G^+ in aqueous solution were 9.0 and 9.2, respectively. The corresponding value for the hydrated β-glucopyranose obtained by the CPMD simulation[5] is 10.2. In going from β-glucopyranose to β-ribofuranose, the total average number of intermolecular H-bonds decreased by only about one. In light of the possibility that one missing hydroxyl group might cause a decrease by about two in this quantity because one hydroxyl group can in principle participate in two H-bonds with water molecules, this implies that, on average, each β-ribofuranose oxygen atom participated in a greater number of intermolecular H-bonds than that of β-glucopyranose. However, the results compared here might be comparable to statistical errors due to the limited time lengths of both the previous ab initio MD simulation of glucopyranose and our present ones.

Next, we examined the ribofuranose−oxygen−water−oxygen (O_W) pair correlation functions, which basically describe the hydration structure of β-ribofuranose. In all of the pair correlation functions (except for the ring oxygen), the positions of the first highest peaks, which mainly arise from the interactions between ribofuranose oxygens and those of first-hydration-shell

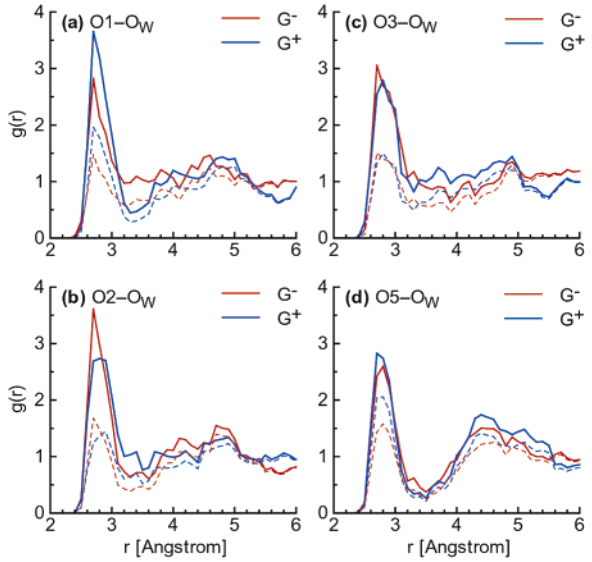

Figure 2. Ribofuranose−oxygen−water−oxygen pair correlation functions (a, O1−O$_W$; b, O2−O$_W$; c, O3−O$_W$; d, O5−O$_W$, where O$_W$ denotes water oxygens). The pair correlation functions were calculated using both the conventional spherical averaging (dashed line) and the *accessible volume* (ref 4) normalization (bold solid line), in which the space around the β-ribofuranose molecule was obtained by the Monte Carlo method. The aim for the latter technique is to eliminate the artifacts resulting from the spherical averaging (ref 4).

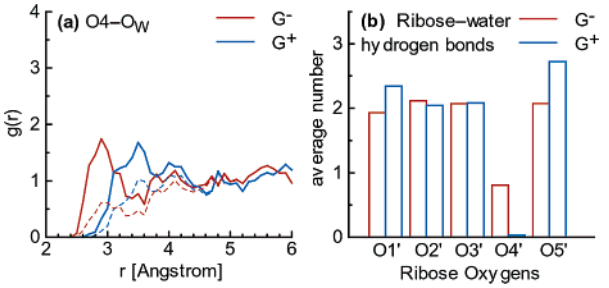

Figure 3. Ring−oxygen−water−oxygen pair correlation functions (a) and the average number of ribofuranose−water intermolecular hydrogen bonds (b). Red and blue indicate G$^-$ and G$^+$, respectively. The atom labeling scheme is the same as that in Figure 1. The criteria for the existence of a hydrogen bond (O$_D$−H···O$_A$) were O$_D$−H ≤ 1.5 Å, H···O$_A$ ≤ 2.4 Å, and ∠O$_D$HO$_A$ > 120°, where O$_D$ and O$_A$ are proton-donor and proton-acceptor oxygens, respectively. The pair correlation functions were calculated using both the conventional spherical averaging (dashed line) and the *accessible volume* (ref 4) normalization (bold solid line), in which the space around the β-ribofuranose molecule was obtained by the Monte Carlo method. The aim for the latter technique is to eliminate the artifacts resulting from the spherical averaging (ref 4).

water molecules, are about 2.7 Å (see Figure 2). However, we found there were slight differences in the depth of the curves following the first peak. For instance, the O1−O$_W$ pair correlation function of G$^+$ shows the relatively deep minimum at ∼3.3 Å, whereas that of G$^-$ does not (Figure 2a). Consistently, the former is characterized by the relatively clear peak centered on ∼4.6 Å as well as the second minimum located at ∼5.7 Å, but such features are not clearly detected in the latter (Figure 2a). This kind of difference between the rotamers is found in the O2−O$_W$ pair correlation functions (Figure 2b), in which in this case the first minimum in the pair correlation function of G$^+$ is less clear. In the O3−O$_W$ pair correlation functions, the first minimum depths in both rotamers are relatively shallow (Figure 2c). According to our analysis by monitoring the trajectories, these observed shallow minima in the 3−4 Å region appeared to arise from somewhat fast making and breaking of intermolecular H-bonds caused by one or two particular water molecules. On the other hand, in contrast with the hydroxyl−oxygen−water−oxygen pair correlation functions, the O5−O$_W$ ones show the best-defined hydration structure, being characterized by the first deep minimum located at ∼3.5 Å and the broad peak centered on ∼4.5 Å that can be assigned to the second hydration shell (Figure 2d). The dependence of the first minimum depth of these pair correlation functions on ribofuranose oxygen is consistent with the idea of *anisotropic solvent structuring*[3] around monosaccharides.

In our ab initio MD simulations, the clearest difference in the hydration structure between the two rotamers was found on the ring oxygen, which is confirmed by the O4−O$_W$ pair correlation functions (Figure 3a). In G$^+$, the position of the first highest peak in the pair correlation function is large (∼3.5 Å), indicating that the ring oxygen of G$^+$ hardly interacted with water molecules in the simulation run. On the other hand, in the case of G$^-$, the position of the first highest peak is about 2.9 Å, showing a small dilation of ≈0.2 Å from the corresponding positions (2.7−2.8 Å) in the other pair correlation functions and thus a slightly weaker ability to form H-bonds compared with the hydroxyl oxygens. The difference in the first peak (Figure 3a) of the ring−oxygen−water−oxygen pair correlation functions between the two rotamers implies that H-bond networks near the ring oxygen were significantly influenced by the orientation of the hydroxymethyl group.

The analysis of the distributions of the average numbers of intermolecular H-bonds was also consistent with the above findings: in G$^-$, the average number of intermolecular H-bonds was 0.8, which means that the ring oxygen participated in one intermolecular H-bond as a proton acceptor in a large number of the configurations, whereas, in G$^+$, the corresponding value was much smaller (0.03) (see also Figure 3b). Certainly, such a small average number of H-bonds for the latter might depend on our criteria used herein. However, it was reported[5] that details of the criteria for H-bonds do not substantially affect a qualitative description of H-bonding properties. To clarify this ambiguity, we recounted the average number of intermolecular H-bonds, using other less restricted criteria:[2,5] O$_D$···O$_A$ ≤ 3.4 Å and ∠O$_D$HO$_A$ > 120°. The number was again small (0.09), which means that the ring oxygen of G$^+$ hardly H-bonded with water molecules. Instead, on the O1 and O5 of the G$^+$ rotamer, the average numbers of intermolecular H-bonds were larger than two (see also Figure 3b). More quantitatively, we found that about 36 and 72% of the configurations were in the form of three intermolecular H-bonds on these sites, respectively, indicating that the anomeric and hydroxymethyl oxygens of G$^+$ tended to attract water molecules somewhat tightly.

To analyze the microscopic origin of the above differences in the hydration structures between the two rotamers, we carefully monitored the H-bond network structure near the ring oxygen of our MD trajectories. From our graphical analyses, we found that, in a large number of the configurations, particular H-bond networks were formed near the ring oxygen; they consisted of two oxygens of β-ribofuranose and three neighboring H-bonded water molecules, where the second-hydration-shell water molecule connected the two first-hydration-shell ones. For instance, in the G$^-$ rotamer, the H-bond network started with the ring oxygen and ended with O2 (Figure 4a), whereas, in the G$^+$ rotamer, the H-bond network started with the anomeric oxygen and ended with the hydroxymethyl one (Figure 4b). Hereafter, we refer to these kinds of H-bond networks on the surface of β-ribofuranose as *circular H-bond networks*.

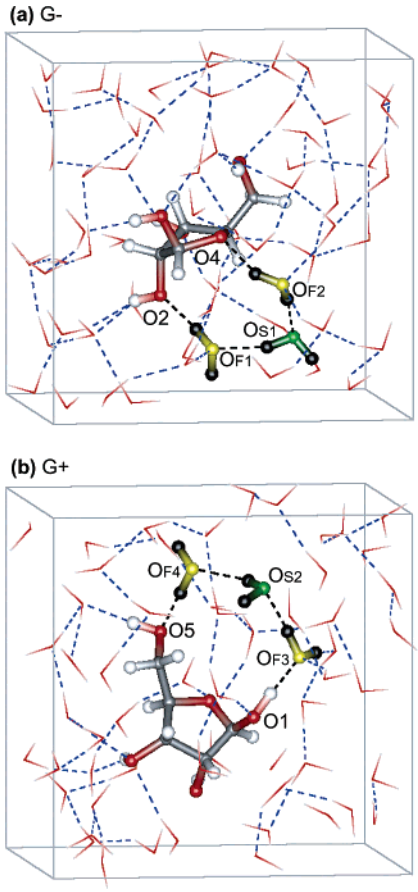

Figure 4. Representative configurations showing the circular hydrogen bond networks near the ring oxygen in the hydrated G^- (a) and G^+ (b) rotamers of β-ribofuranose. These were sampled from our ab initio MD trajectories. Hydrogen bonds in the circular hydrogen bond networks are colored separately by black, while others, by blue. The three water molecules that form the circular hydrogen bond networks are represented by ball-and-sticks, where oxygens of the first- and second-hydration-shell water molecules are colored separated by yellow and green with hydrogens black, as well as labeled by the subscripts F and S, respectively. β-Ribofuranose and the other water molecules are represented by ball-and-sticks and sticks, respectively (carbon atoms, gray; oxygens, red; hydrogens, white). For our molecular visualization, we used gOpenMol, version 2.32 (ref 92), throughout the paper.

This definition is very similar to the idea of *circular hydrogen bonds*,[11] which was introduced by Saenger to describe the interactions between cyclodextrin and water molecules. In that study, all oxygens in H-bonded cycles *must be* connected by either inter- or intramolecular H-bonds.[11] However, our definition of a circular H-bond network seems slightly relaxed compared to the usage that was originally intended to describe H-bonded cycles in the cyclodextrin hexahydrate.[11−13] In our definition, two sugar oxygens at the termini of the circular H-bond network *do not need* to have an intramolecular H-bond between them. On the other hand, we also note that it was originally pointed out[11] that circular H-bonds might play a role on the surfaces of biological molecules in aqueous solution. In this sense, the meaning of *circular H-bonds* seems almost equivalent to our definition of a *circular H-bond network*; however, to avoid possible unnecessary confusion, in this paper, we use circular H-bond networks.

To examine more quantitatively the nature of these circular H-bond networks, we introduced an *H-bonding function*, which is unity if a particular pair of oxygens forms an H-bond and decays to zero as they deviate from a predefined condition for H-bonds. Our H-bonding function is similar to that of ref 83 and defined by $H(t) = R(t)\cdot A(t)$, where $R(t)$ is unity if $d(t) \le d_c$ and otherwise $\exp[-(d(t) - d_c)^2/2\sigma_r^2]$, while $A(t)$ is unity if $\theta(t) > \theta_c$ and otherwise $\exp[-(\theta(t) - \theta_c)^2/2\sigma_\theta^2]$. Here, $d(t)$ and $\theta(t)$ are the instantaneous H$\cdot\cdot\cdot$O$_A$ distance and O$_D$−H−O$_A$ angle, respectively, and in our present work, d_c, θ_c, σ_r, and σ_θ were 2.4 Å, 120°, 0.2 Å, and 10°, respectively. In the case of an H-bond network, in this paper, we simply assumed an H-bonding function for the H-bond network as a product of all H-bonding functions for the H-bonds that construct the network.

From the viewpoint of static properties, an MD trajectory can be regarded as a sampling of configurations from a thermodynamic ensemble. In this picture, about 50 and 70% of the configurations were in the form of the five-membered circular H-bond networks like parts a and b of Figure 4, respectively, when the condition that the H-bonding function be not less than 0.8 was used for the definition for the existence of H-bonds. The existence of the former circular H-bond network (Figure 4b) during the simulation suggests that the ring oxygen was partially shielded from the water molecules by the network that connected the anomeric and hydroxymethyl oxygens, which explains why the ring oxygen of G^+ hardly H-bonded with water molecules.

The calculations of the H-bonding functions in these circular H-bond networks provide a more detailed analysis of the dynamics of the making and breaking of the networks. In the circular H-bond network that connected O2 and O4 of G^-, the breaks of this network occurred at either the ribofuranose−water (at ∼3.0−3.5 ps in O2$\cdot\cdot\cdot$O$_{F1}$ and 5.2−6.0 ps in O$_{F2}\cdot\cdot\cdot$O4) or the water−water (at ∼4.3−5.0 ps in O$_{S1}\cdot\cdot\cdot$O$_{F2}$) H-bonds (Figure 5a). On the other hand, the circular H-bond network that connected O1 and O5 of G^+ lived longer (from ∼1.6 ps to the end of the simulation, if we neglect the relatively short breaks, see Figure 5b), although the limited length of our simulation did not allow us to obtain its lifetime. This longer-lived circular H-bond network in G^+ might be enhanced by the existence of the long-lived (more than 5 ps, see Figure 5b) intermolecular H-bonds at O1 and O5.

To explain these relatively long intermolecular H-bonds of O1 and O5 of the G^+ rotamer, we examined the electronic properties of the OH groups of β-ribofuranose. To this end, we used the centers of the maximally localized Wannier functions,[84] which were computed at every 10 steps in our simulations (details of maximally localized Wannier functions and a variety of applications can be found in the literature[84,85]). In our analysis, The Wannier functions that are close to an OH group are classified into a covalent OH-bond orbital and two lone-pair orbitals, and hereafter, we refer to the centers of these Wannier functions as CWFC and LPWFC, respectively (for the graphical representations of these centers, see Figure 6). For comparison, we also calculated the electronic properties of seven water molecules well apart from β-ribofuranose during our simulations (four water molecules from the simulation of G^- and three from that of G^+); the average O−CWFC, CWFC−H, and O−LPWFC distances were 0.510, 0.502, and 0.333 Å, respectively (averaged over 6200 configurations). Now, the first thing we find in Table 1 is that the average CWFC−H1 distance in G^+ is the longest one (0.518 Å) among all CWFC−H distances, being about 3% longer than that of a water molecule in the liquid (0.502 Å), indicating that H1 of G^+ was most positively charged among the hydrogen atoms of the OH groups and that it acted as a good proton donor. Consistently, the average O1−CWFC distance in G^+ is 0.504 Å (Table 1), which is shorter by 0.006 Å than the corresponding distance of water in the liquid (0.510 Å), suggesting that, in G^+, H1 lost more electrons in favor of

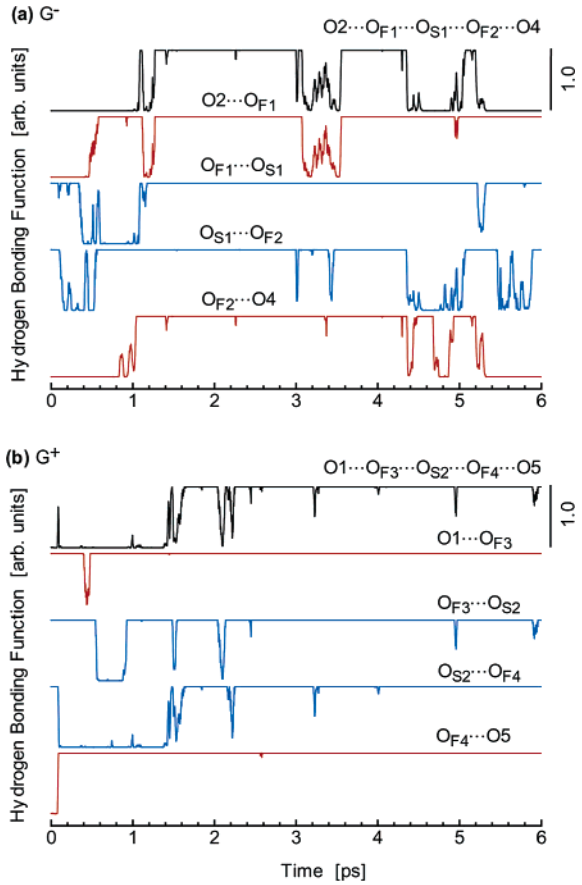

Figure 5. Hydrogen bonding functions for the circular hydrogen bond networks near the ring oxygen obtained from the simulations of the G^- (a) and G^+ (b) rotamers. O_F and O_S denote the oxygens of the first- and second-hydration-shell water molecules, respectively. The notations are the same as those in Figure 4. Hydrogen bonding functions for the circular hydrogen bond networks are colored black, whereas those between β-ribofuranose and the first-hydration-shell-water oxygens are indicated by red and those between the first- and second-hydration-shell-water oxygens are indicated by blue. For the definition of hydrogen bonding functions, see the text.

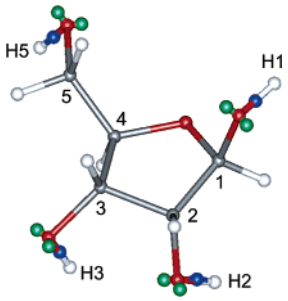

Figure 6. Centers of the maximally localized Wannier functions associated with the covalent OH-bond (blue) and lone-pair (green) orbitals of the hydroxyl and hydroxymethyl groups of β-ribofuranose. In the β-ribofuranose molecule with the atom labeling, carbon atoms are colored gray, oxygens red, and hydrogens white. The conformer shown here is the G^+ rotamer of β-ribofuranose in the north form.

the O1 compared with hydrogen atoms of a water molecule in the liquid. The above findings are consistent with the observed long-lived intermolecular H-bonds (see the H-bonding function for O1···O_{F3} in Figure 5b). The second finding in Table 1 is that one of the O5−LPWFC distances of G^+ is the longest (0.338 Å) (the other O5−LPWFC distance is also relatively long; see Table 1), which is about 1.5% larger than that of a water molecule in the liquid (0.333 Å). This means that, because

TABLE 1: Electronic Properties of the OH Groups of β-Ribofuranose in Aqueous Solution Obtained by the ab Initio MD Simulations[a]

rotamer	OH group	O−CWFC (Å)	CWFC−H (Å)	O−LPWFC (Å)		θ_{LP} (deg)
G^-	O1−H1	0.509	0.511	0.314	0.318	122.0
	O2−H2	0.506	0.513	0.318	0.328	120.4
	O3−H3	0.508	0.509	0.320	0.323	121.3
	O5−H5	0.514	0.497	0.331	0.321	120.6
G^+	O1−H1	0.504	0.518	0.321	0.330	120.5
	O2−H2	0.511	0.509	0.327	0.315	122.5
	O3−H3	0.511	0.503	0.316	0.327	120.2
	O5−H5	0.507	0.512	0.327	0.338	119.0

[a] CWFC and LPWFC denote the centers of the maximally localized Wannier functions associated with the covalent OH-bond and lone-pair orbitals belonging to the OH groups of β-ribofuranose, respectively (see also Figure 6). Each value for θ_{LP} is the LPWFC−O−LPWFC angle belonging to each OH group of β-ribofuranose. Data were obtained by averaging over 6200 configurations.

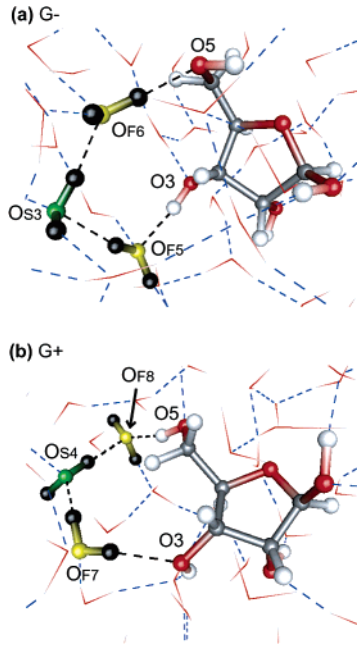

Figure 7. Representative configurations showing the circular hydrogen bond networks connecting O3 and O5 in the hydrated G^- (a) and G^+ (b) rotamers of β-ribofuranose. These were sampled from our ab initio MD trajectories. Hydrogen bond networks of interest are colored separately by black, while others, by blue. Three water molecules that form the circular hydrogen bond networks are represented by ball-and-sticks, where oxygens of the first- and second-hydration-shell water molecules are colored separately by yellow and green with hydrogens black, as well as labeled by the subscripts F and S, respectively. β-Ribofuranose and other water molecules are represented by ball-and-sticks and sticks, respectively (carbon atoms, gray; oxygens, red; hydrogens, white).

of the ribofuranose−water interaction, this lone-pair Wannier orbital was continuously pulled out by the first-hydration-shell water molecule, suggesting that O5 of G^+ acted as a good proton acceptor. This is also consistent with the observed long-lived intermolecular H-bonds between O5 of G^+ and the first-hydration-shell water molecule (see the H-bonding function for O_{F4}···O5 in Figure 5b).

Other circular H-bond networks we observed in our simulations were those connecting O3 and O5 (see Figure 7). The arrangements of H-bonds in circular H-bond networks between the rotamers were different (we will discuss this issue later). The calculations of the H-bonding functions for these circular H-bond networks show that the circular H-bond network shown

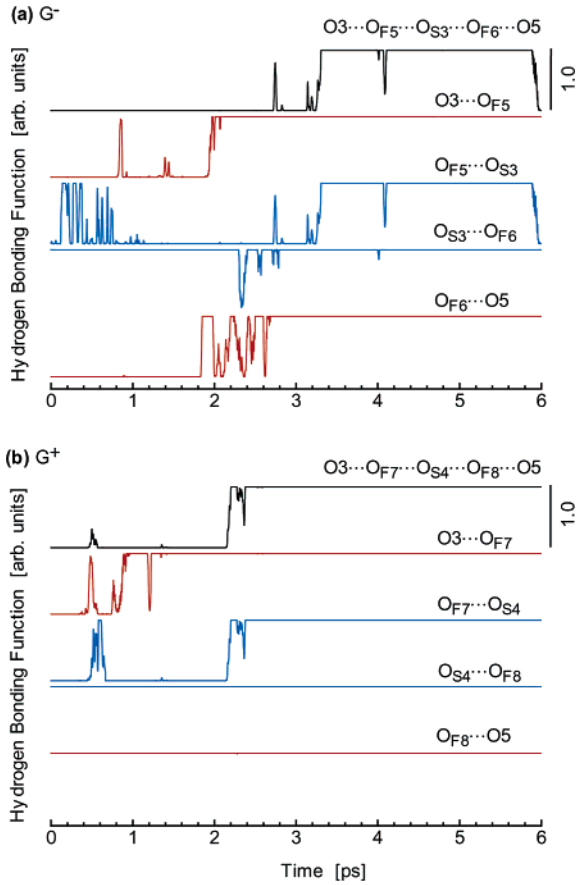

Figure 8. Hydrogen bonding functions for the circular hydrogen bond networks connecting O3 and O5 obtained from the simulations of the G^- (a) and G^+ (b) rotamers. Here, O_F and O_S denote oxygens of the first- and second-hydration-shell waters, respectively. For the definition of hydrogen bonding functions, see the text.

in Figure 7b lived longer than that in Figure 7a (Figure 8). Furthermore, using the information about the H-bonding function shown in Figure 5b, we found that, in about 60% of the configurations, the hydroxymethyl oxygen of the G^+ rotamer simultaneously participated in two circular H-bond networks: one connecting to O1 (Figure 4b) and the other connecting to O3 (Figure 7b). This indicates that the hydration structure near the hydroxymethyl group of G^+ was more rigid than that of G^-. To explain this point more clearly, we again examined the electronic properties of the O5H5 group of the G^+ rotamer. Since, in G^+, O5 acted as a proton donor in the circular H-bond network connecting O5 and O3 (Figure 7b), we looked at the distance between H5 and the center of the covalent O5H5-bond Wannier function. The average CWFC−H5 distance is relatively long (0.512 Å) (Table 1), implying that H5 of G^+ lost electrons in favor of O5 and was therefore relatively positively charged, possibly because the lone-pair orbitals of O5 were continuously pulled out, as mentioned. This is consistent with the observed long-lived O5• • •O_{F8} intermolecular H-bonds (see Figure 8b).

Now, we turn to the geometrical aspects of the circular H-bond networks observed in our simulations and their arrangements of H-bonds. The geometries of some of the circular H-bond networks were highly distorted from that of the cyclic water pentamer. The average angles of $O_{F1}-O_{S1}-O_{F2}$, $O_{F3}-O_{S2}-O_{F4}$, $O_{F5}-O_{S3}-O_{F6}$, and $O_{F7}-O_{S4}-O_{F8}$ were 109.0, 121.3, 108.8, and 121.3°, respectively (for the notations of these oxygen atoms, see Figures 4a, 4b, 7a, and 7b, respectively), which were obtained using the configurations that strictly satisfied our criteria for the existence of a circular H-bond network. In

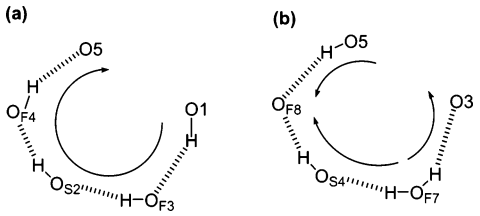

Figure 9. Schematic illustrations of the homodromic (a) and antidromic (b) arrangements of hydrogen bonds observed in our circular hydrogen bond networks in the ab initio MD trajectory. Note that not all of the arrangements are presented here. The arrangements in parts a and b schematically represent the circular hydrogen bond networks in Figures 4b and 7b, respectively. Dotted lines indicate hydrogen bonds. The arrows denote the directions of hydrogen bonds.

particular, the second and forth values (121.3°) are roughly 10% larger than the average O−O−O angle in the cyclic water pentamer[86−89] (108°) or the tetrahedral angle (109°). One of the reasons for these distortions is that the average distances between two ribofuranose oxygens are large (in G^+, the average O1−O5 and O3−O5 distances were 4.7 and 4.6 Å, respectively) compared with a typical H-bonded oxygen−oxygen one (2.8 Å).

To shed light on the physical origin of these geometrical distortions observed in some of the circular H-bond networks (i.e., those shown in Figures 4b and 7b), we examined the geometric and electronic properties of the first-hydration-shell water molecules in these relatively long-lived circular H-bond networks. Note that the arrangements of H-bonds in the former and latter circular H-bond networks were *homodromic* (which means that all H-bonding patterns run in the same direction) and *antidromic*, respectively, which are schematically illustrated in parts a and b of Figure 9, respectively. More specifically, the water molecules indicated by O_{F4} and O_{F3} in Figure 4 were the first-hydration-shell water molecules that, in a large number of the configurations, acted as a donor and an acceptor, respectively, in the circular H-bond network in a homodromic arrangement, whereas those indicated by O_{F7} and O_{F8} in Figure 7 are the first-hydration-shell water molecules that, in a large number of the configurations, acted as a double donor and double acceptor, respectively, in the circular H-bond network in an antidromic arrangement. Hereafter, we refer to these water molecules as F_D, F_A, F_{DD}, and F_{AA}, respectively.

First, we found that the average LPWFC−O−LPWFC angle (θ_{LP}) of the proton-donating water molecules in the first hydration shell (F_D and F_{DD}) was larger by about 2.5° than that of the proton-accepting water molecules in the first hydration shell (F_A and F_{AA}) (see also Table 2). Furthermore, the former value is also slightly larger (about 1%) than that of a nonhydration water molecule (Table 2). Second, the average θ_{LP} value of F_{AA} was the smallest one (117.5°) among these four water molecules and was smaller by roughly 1% than that of nonhydration water molecules (119.2°), indicating that the directions of the lone-pair orbitals of F_{AA} were slightly narrowed because F_{AA} acted as a double acceptor in the relatively long-lived circular H-bond network. Similar decreases in θ_{LP} were reported for first-hydration-shell water molecules of cations.[90,91] Third, the CWFC−O−CWFC angle (θ_C) of F_{AA} (103.1°) was slightly larger than that of a nonhydration water molecule (102.3°). Consistently, the H−O−H angle of F_{AA} (105.2°) was also slightly larger than that of nonhydration water (104.4°). On the other hand, since the hydrogen atoms of the other water molecules (that is, F_D, F_{DD}, and F_A) were embedded in the circular H-bond networks, the H−O−H angle and θ_C of these water molecules appeared

TABLE 2: Geometric and Electronic Properties of the First-Hydration-Shell Water Molecules in Our Circular Hydrogen Bond Networks[a]

	H−O−H (deg)	θ_C (deg)	θ_{LP} (deg)
F_D	104.4	102.0	120.4
F_A	102.4	101.9	118.0
F_{DD}	103.9	101.8	120.2
F_{AA}	105.2	103.1	117.5
nonhydration water[b]	104.4	102.3	119.2

[a] The angles θ_C and θ_{LP} are the LPWFC−O−LPWFC and CWFC−O−CWFC ones, respectively, where CWFC and LPWFC denote the centers of the maximally localized Wannier functions associated with the covalent OH-bond and lone-pair orbitals of the water molecules in our circular hydrogen bond networks (see also Figure 6), respectively. F_D and F_A denote the first-hydration-shell water molecules that, in a large number of the configurations, acted as a donor and an acceptor, respectively, in the circular H-bond network in a homodromic arrangement, whereas F_{DD} and F_{AA} denote those that, in a large number of the configurations, acted as a double donor and a double acceptor, respectively, in the circular H-bond network in an antidromic arrangement. More specifically, F_D and F_A are the water molecules indicated by O_{F4} and O_{F3} in Figure 4b, whereas F_{DD} and F_{AA} are those indicated by O_{F7} and O_{F8} in Figure 7b. For the schematic illustrations of these arrangements of H-bonds, see also Figure 9. Data were obtained by averaging over the last 5000 configurations. [b] Data were obtained by averaging over 6200 configurations of seven water molecules well apart from β-ribofuranose (four water molecules from the simulation of G^- and three from that of G^+).

(more or less) slightly narrower than or comparable to those of nonhydration water molecules (Table 2).

To further investigate the electronic properties of these water molecules in the first hydration shell, we calculated the dipole moments of the first-hydration-shell water molecules in the circular H-bond networks (F_D, F_A, F_{DD}, and F_{AA}), using the positions of the ions and the centers of the maximally localized Wannier functions. The average value of the dipole moment of the proton-accepting first-hydration-shell water molecules (F_A and F_{AA}) was about 3.26 D, which increased by about 0.3 D from that of liquid water (2.95 D) (see also Figure 10). These values for F_A and F_{AA} are comparable to those from first-hydration-shell water molecules of cations (for the hydration shell of a magnesium ion,[90] 3.3 D; for that of a calcium ion,[91] 3.4−3.5 D). These increases in the water molecule dipole moment were primarily due to the decreases in θ_{LP} of these water molecules (see Table 2). Moreover, the distribution of the dipole moment of the double proton-accepting first-hydration-shell water molecule (F_{AA}) is relatively sharp (Figure 10). On the other hand, the dipole moments of F_D and F_{DD} did not significantly change: The distribution of the dipole moment of the proton-donating first-hydration-shell water molecule (F_D) is characterized by the relatively sharp peak at about 2.85 D (slightly smaller than that of liquid water) and the shoulder at about 3.45 D (Figure 10). The distribution of the double proton-donating first-hydration-shell water molecule (F_{DD}) has the broader width at the half-maximum than the one for F_D and is characterized by the maximum peak at about 3.05 D, which is close to that of liquid water (Figure 10). The difference between F_D and F_{DD} appeared to be attributed to the slightly smaller angles (the H−O−H angle, θ_C, and θ_{LP}) of F_{DD} than those of F_D (see Table 2).

These analyses of the geometric and electronic properties of the first-hydration-shell water molecules in the circular H-bond networks implies that the H-bond networks on the surface of β-ribofuranose were slightly distorted from the H-bond network structure of pure liquid water. Furthermore, looking again at the centers of the Wannier functions associated with the lone-pair orbitals of the OH groups of β-ribofuranose (Table 1), we found three features: First, owing to the H-bonding, two LPWFCs in OH groups of β-ribofuranose were not completely symmetrically located from the closest oxygen ion. Second, the average O−LPWFC distance in the OH groups was 0.323 Å, being 0.01 Å shorter than that of a water molecule in the liquid water (0.333 Å). Third, owing to the shorter O−LPWFC distance, the average θ_{LP} in the OH groups of β-ribofuranose was about 1.3% larger (120.8°) than that of a water molecule in the liquid (119.2°). These features might have nonnegligible effects on the arrangements of H-bonds of water molecules on the surface of β-ribofuranose. Combining our analyses of the geometric and electronic properties of the first-hydration-shell water molecules and the OH groups of β-ribofuranose, we believe that circular H-bond networks on the surface of β-ribofuranose are real and that they exist at least on the time scale of several picoseconds. Moreover, it is likely that H-bonds of water molecules on the surface of β-ribofuranose can be arranged in a different way, for example, in an antidromic arrangement, though, in the cyclic water pentamer, the most favored arrangement of H-bonds is homodromic.[86−89]

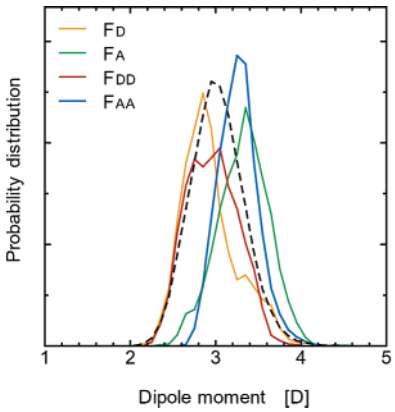

Figure 10. Distributions of the dipole moments of the first-hydration-shell water molecules. F_D (orange) and F_A (green) denote the first-hydration-shell water molecules that, in a large number of the configurations, acted as a donor and an acceptor, respectively, in the circular H-bond network in a homodromic arrangement, whereas F_{DD} (red) and F_{AA} (blue) denote the ones that, in a large number of the configurations, acted as a double donor and a double acceptor, respectively, in the circular H-bond network in an antidromic arrangement. More specifically, F_D and F_A are the water molecules indicated by O_{F4} and O_{F3} in Figure 4b, whereas F_{DD} and F_{AA} are those indicated by O_{F7} and O_{F8} in Figure 7b. For the schematic illustrations of these arrangements of H-bonds, see also Figure 9. Data were obtained by considering the last 5000 configurations. The dashed line is the distribution of the dipole moments of seven water molecules well apart from β-ribofuranose (four water molecules from the simulation of G^- and three from that of G^+), which was obtained by considering 6200 configurations.

Conclusions

In conclusion, we examined the H-bond network structure on the surface of β-ribofuranose in aqueous solution using ab initio MD simulations. In particular, we investigated the circular H-bond networks involving two β-ribofuranose oxygens and three water molecules. In our simulations, the circular H-bond networks near the ring oxygen of β-ribofuranose were significantly influenced by the orientation of the hydroxymethyl group: In the G^+ rotamer, the ring oxygen hardly H-bonded with water molecules during our simulation run (6 ps) because the ring oxygen was partially shielded by the circular H-bond network connecting O1 and O5 in a large number of the

configurations. In the G^- rotamer, the circular H-bond network connecting O2 and the ring oxygen was formed in about half the configurations. These indicate that the concept of circular H-bond networks may be useful in explaining the difference in the hydration structure between the hydroxymethyl rotamers of β-ribofuranose. Besides, the above difference observed in our simulations may have implications for the stabilities and the low-frequency dynamics of the hydroxymethyl rotamers of β-ribofuranose in aqueous solution and possibly for modeling the hydration of monosaccharides.

To investigate the microscopic polarization effects created by the interactions between β-ribofuranose and water molecules, we used the method of maximally localized Wannier functions. The analysis of the localized Wannier orbitals showed that, in the OH group of β-ribofuranose that acted as a proton donor in the long-lived intermolecular H-bond, the distance between the hydrogen atom and the center of the covalent OH-bond Wannier orbital was about 3% larger than that of a water molecule in the liquid. Furthermore, whereas the dipole moments of the proton-donating first-hydration-shell water molecules did not significantly change, those of the proton-accepting first-hydration-shell water molecules in our well-defined circular H-bond networks increased by about 0.3 D compared with that of liquid water, which is comparable to those of the hydration shells of cations.[90,91] These enhancements were primarily due to the decreases in the angle between the two vectors of the centers of the lone-pair Wannier orbitals from the oxygen atom (the LPWFC−O−LPWFC angles). Our analysis presented here using the centers of the localized Wannier orbitals implies that circular H-bond networks cannot be fully explained from a simple geometrical point of view.

These enhancements of the dipole moments of the water molecules of our circular H-bond networks appeared to be a possible origin for the distortions of the local H-bond network structures on the surface of β-ribofuranose in aqueous solution and their somewhat irregular (i.e., antidromic) arrangements of H-bonds. The above enhancements also suggest relatively strong polarization effects induced by the interactions between OH groups of monosaccharides and surrounding water molecules, which possibly affects the dynamical properties of the H-bond network of liquid water around monosaccharides and may have implications for their biological functions. Also, our analysis implies that relatively strong intermolecular H-bonds between the OH groups of β-ribofuranose and first-hydration-shell water molecules might play a role in the formation of circular H-bond networks, when two water molecules in the first hydration shell are connected by a second-hydration-shell one. On the other hand, the enhancements of the dipole moments of water molecules in circular hydrogen bond networks might depend on their lifetimes.

While our present work suggests circular H-bond networks on the surface of β-ribofuranose on the time scale of several picoseconds, we are also aware of the limitations of the present work, such as the system size, the length of our simulation run, and the performance of density functional theory combined with the BLYP functional. In particular, very recent studies[80,81,93] about the performance of density functional theory for ab initio MD simulations of liquid water pointed out that the BLYP functional tends to make liquid water more structured and less diffusive at ambient temperatures. The implication of these studies for our study is that lifetimes of circular H-bond networks may be difficult to accurately predict. Despite this, we believe that theoretical studies of the hydration of monosaccharides by ab initio MD simulations are necessary and remain a challenge.

Acknowledgment. We thank Hiromi Kotoku for helping in the simulations. Our ab initio molecular dynamics simulations were performed on the Hitachi SR8000 instrument of Information Technology Center, University of Tokyo.

References and Notes

(1) Kabayama, M.; Patterson, D. *Can. J. Chem.* **1958**, *36*, 563−575.
(2) Schmidt, R. K.; Karplus. M.; Brady, J. W. *J. Am. Chem. Soc.* **1996**, *118*, 541−546.
(3) Liu, Q.; Brady, J. W. *J. Am. Chem. Soc.* **1996**, *118*, 12276−12286.
(4) Leroux, B.; Bizot, H.; Brady, J. W.; Tran, V. *Chem. Phys.* **1997**, *216*, 349−363.
(5) Molteni, C.; Parrinello, M. *J. Am. Chem. Soc.* **1998**, *120*, 2168−2171.
(6) Franks, F. *Pure Appl. Chem.* **1987**, *59*, 1189−1202 and references therein.
(7) Uedaira, H.; Ikura, M.; Uedaira, H. *Bull. Chem. Soc. Jpn.* **1989**, *62*, 1−4 and references therein.
(8) Cheetham, N. W. H.; Lam, K. *Aust. J. Chem.* **1996**, *49*, 365−369.
(9) Warner, D. T. *Nature* **1962**, *196*, 1055−1058.
(10) (a) Galema, S. A.; Blandamer, M. J.; Engberts, J. B. F. N. *J. Am. Chem. Soc.* **1990**, *112*, 9665−9666. (b) Galema, S. A.; Høiland, H. *J. Phys. Chem.* **1991**, *95*, 5321−5326. (c) Galema, S. A.; Engberts. J. B. F. N.; Høiland, H.; Førland, G. M. *J. Phys. Chem.* **1993**, *97*, 6885−6889. (d) Galema, S. A.; Howard, E.; Engberts, J. B. F. N.; Grigera, J. R. *Carbohydr. Res.* **1994**, *126*, 215−225.
(11) Saenger, W. *Nature* **1979**, *279*, 343−344.
(12) Steiner, T. *Angew. Chem., Int. Ed.* **2002**, *41*, 48−76.
(13) Saenger, W.; Steiner, T. *Acta Crystallogr., Sect. A* **1998**, *54*, 798−805.
(14) (a) Brady, J. W. *J. Am. Chem. Soc.* **1986**, *108*, 8153−8160. (b) Brady, J. W. *Carbohydr. Res.* **1987**, *165*, 306−312.
(15) Ha, S. N.; Giammona, A.; Field, M.; Brady, J. W. *Carbohydr. Res.* **1988**, *180*, 207−221.
(16) Polavarapu, P. L.; Ewig, C. S. *J. Comput. Chem.* **1992**, *13*, 1255−1261.
(17) Salzner, U.; von Rague Schleyer, P. *J. Org. Chem.* **1994**, *59*, 2138−2155.
(18) Barrows, S. E.; Dulles, F. J.; Cramer, C. J.; French, A. D.; Truhlar, D. G. *Carbohydr. Res.* **1995**, *276*, 219−251.
(19) Dowd, M. K.; French, A. D.; Reilly, P. J. *Carbohydr. Res.* **1994**, *264*, 1−19.
(20) Csonka, G. I.; Éliás, K.; Csizmadia, I. G. *Chem. Phys. Lett.* **1996**, *257*, 49−60.
(21) Jebber, K. A.; Zhang, K.; Cassady, C. J.; Chung-Philips, A. *J. Am. Chem. Soc.* **1996**, *118*, 10515−10524.
(22) Brown, J. A.; Wladkowski, B. D. *J. Am. Chem. Soc*. **1996**, *118*, 1190−1193.
(23) Csonka, G. I.; Kolossváry, I.; Császár, P.; Éliás, K.; Csizmadia, I. G. *THEOCHEM* **1997**, *395*−*396*, 29−40.
(24) Damm, W.; Frontera, A.; Tirado-Rives, J.; Jorgensen, W. L. *J. Comput. Chem.* **1997**, *18*, 1955−1970.
(25) Simmerling, C.; Fox, T.; Kollman, P. A. *J. Am. Chem. Soc*. **1998**, *120*, 5771−5782.
(26) Barrows, S. E.; Storer, J. W.; Cramer, C. J.; French, A. D.; Truhlar, D. G. *J. Comput. Chem.* **1998**, *19*, 1111−1129.
(27) Wladkowski, B. D.; Chenoweth, S. A.; Jones, K. E.; Brown, J. W. *J. Phys. Chem. A* **1998**, *102*, 5086−5092.
(28) Csonka, G. I. *THEOCHEM* **2002**, *584*, 1−4.
(29) Lii, J.-H.; Chen, K.-H.; Aligner, N. L. *J. Comput. Chem.* **2003**, *24*, 1504−1513 and references therein.
(30) Appell, M.; Strati, G.; Willett, J. L.; Momany, F. A. *Carbohydr. Res.* **2004**, *339*, 537−551.
(31) Kouwijzer, M. L. C. E.; van Eijck, B. P.; Kroes, S. J.; Kroon, J. *J. Comput. Chem.* **1993**, *14*, 1281−1289.
(32) Kouwijzer, M. L. C. E.; van Eijck, B. P.; Koojiman, H.; Kroon, J. *Acta Crystallogr., Sect. B* **1995**, *51*, 209−220.
(33) Molteni, C.; Parrinello, M. *Chem. Phys. Lett.* **1997**, *275*, 409−413.
(34) Cramer, C. J.; Truhlar, D. G. *J. Am. Chem. Soc.* **1993**, *115*, 5745−5753.
(35) Zuccarello, F.; Buemi, G. *Carbohydr. Res.* **1995**, *273*, 129−145.
(36) Cramer, C. J.; Truhlar, D. G.; French, A. D. *Carbohydr. Res.* **1997**, *298*, 1−14.
(37) Ma, B.; Schaefer, H. F., III; Allinger, N. L. *J. Am. Chem. Soc.* **1998**, *120*, 3411−3422.

(38) Hoffmann, M.; Rychlewski, J. *J. Am. Chem. Soc.* **2001**, *123*, 2308−2316.
(39) Momany, F. A.; Appell, M.; Strati, G.; Willett, J. L. *Carbohydr. Res.* **2004**, *339*, 553−567.
(40) Klein, R. A. *J. Am. Chem. Soc.* **2002**, *124*, 13931−13937.
(41) Suzuki, T.; Sota, T. *J. Chem. Phys.* **2003**, *119*, 10133−10137.
(42) Brady, J. W. *J. Am. Chem. Soc.* **1989**, *111*, 5155−5165.
(43) Van Eijck, B. P.; Kroon-Batenburg, L. M. J.; Kroon, J. *J. Mol. Struct.* **1990**, *237*, 315−325.
(44) Ha, S.; Gao, J.; Tidor, B.; Brady, J. W.; Karplus, M. *J. Am. Chem. Soc.* **1991**, *113*, 1553−1557.
(45) Van Eijck, B. P.; Hooft, R. W. W.; Kroon, J. *J. Phys. Chem.* **1993**, *97*, 12093−12099.
(46) Glennon, T. M.; Zheng, Y.-J.; Le Grand, S. M.; Schutzberg, B. A.; Merz, K. M., Jr. *J. Comput. Chem.* **1994**, *15*, 1019−1040.
(47) Corchado, J. C.; Sánchez, M. L.; Aguilar, M. A. *J. Am. Chem. Soc.* **2004**, *126*, 7311−7319.
(48) Kirschner, K. N.; Woods, R. J. *Proc. Natl. Acad. Sci. U.S.A.* **2001**, *98*, 10541−10545.
(49) Serianni. A. S.; Chipman, D. M. *J. Am. Chem. Soc.* **1987**, *109*, 5297−5303.
(50) Kline, P. C.; Serianni, A. S. *J. Am. Chem. Soc.* **1990**, *112*, 7373−7381.
(51) Podlasek, C. A.; Stripe, W. A.; Carmichael, I.; Shang, M.; Basu, B.; Serianni, A. S. *J. Am. Chem. Soc.* **1996**, *118*, 1413−1425.
(52) Church, T. J.; Carmichael, I.; Serianni, A. S. *J. Am. Chem. Soc.* **1997**, *119*, 8946−8964.
(53) Kennedy, J.; Wu, J.; Drew, K.; Carmichael, I.; Serianni, A. S. *J. Am. Chem. Soc.* **1997**, *119*, 8933−8945.
(54) Brameld, K. A.; Goddard, W. A., III. *J. Am. Chem. Soc.* **1999**, *121*, 985−993.
(55) Gordon, M. T.; Lowary, T. L.; Hadad, C. M. *J. Am. Chem. Soc.* **1999**, *121*, 9682−9692.
(56) Coloran, F.; Zhu, Y.; Osborn, J.; Carmichael, I.; Serianni, A. S. *J. Am. Chem. Soc.* **2000**, *122*, 6435−6448.
(57) Cloran, F.; Carmichael, I.; Serianni, A. S. *J. Am. Chem. Soc.* **2001**, *123*, 4781−4791 and references therein.
(58) Harvey, S. C.; Prabhakaran, M. *J. Phys. Chem.* **1987**, *91*, 4799−4801.
(59) Van Eijck, B. P.; Kroon, J. *J. Mol. Struct.* **1989**, *195*, 133−146.
(60) Plavec, J.; Tong, W.; Chattopadhyaya, J. *J. Am. Chem. Soc.* **1993**, *115*, 9734−9746.
(61) Tomimoto, M.; Go, N. *J. Phys. Chem.* **1995**, *99*, 563−577.
(62) Gabb, H. A.; Lavery, R.; Prévost, C. *J. Comput. Chem.* **1995**, *16*, 667−680.
(63) Grůza, J.; Koča, J.; Pérez, S.; Imberty, A. *THEOCHEM* **1998**, *424*, 269−280.
(64) Dejaegere, A. P.; Case, D. A. *J. Phys. Chem. A* **1998**, *102*, 5280−5289.
(65) Houseknecht, J. B.; McCarren, P. R.; Lowary, T. L.; Hadad, C. M. *J. Am. Chem. Soc.* **2001**, *123*, 8811−8824.
(66) Guler, L. P.; Yu, Y.-Q.; Kenttämaa, H. I. *J. Phys. Chem. A* **2002**, *106*, 6754−6764.
(67) Houseknecht, J. B.; Altona, C.; Hadad, C. M.; Lowary, T. L. *J. Org. Chem.* **2002**, *67*, 4647−4651.
(68) Boero, M.; Terakura, K.; Tateno, M. *J. Am. Chem. Soc.* **2002**, *124*, 8949−8957.
(69) To our knowledge, only the trajectory-averaged hydration structure around β-ribofuranose was reported in ref 59.
(70) (a) Car, R.; Parrinello, M. *Phys. Rev. Lett.* **1985**, *55*, 2471−2474. (b) Parrinello, M. *Solid State Commun.* **1997**, *102*, 107−120. (c) Marx, D.; Hutter, J. In *Modern Methods and Algorithms of Quantum Chemistry*; Grotendorst, J., Ed.; NIC, FZ: Jülich, Germany, 2000; pp 301−449; see also http://www.theochem.ruhr-uni-bochum.de/research/marx/cprev.en.html.
(71) (a) Altonoa, C.; Sundaralingam, M. *J. Am. Chem. Soc.* **1972**, *94*, 8205−8212. (b) Rao, S. T.; Westhof, E.; Sundaralingam, M. *Acta Crystallogr., Sect. A* **1981**, *37*, 421−425.
(72) (a) Hohenberg, P.; Kohn, W. *Phys. Rev.* **1964**, *136*, B864−B871. (b) Kohn, W.; Sham, L. J. *Phys. Rev.* **1965**, *140*, A1133−A1138. (c) Parr, R. G.; Yang, W. In *Density-Functional Theory of Atoms and Molecules*; Breslow, R., Goodenough, J. B., Halpern, J., Rowlingson, J. S., Eds.; The International Series of Monographs on Chemistry 16; Oxford University Press: New York, 1989.
(73) (a) Becke, A. D. *Phys. Rev. A* **1988**, *38*, 3098−3100. (b) Lee, C.; Yang, W.; Parr, R. G. *Phys. Rev. B* **1988**, *37*, 785−789.
(74) (a) Sprik, M.; Hutter, J.; Parrinello, M. *J. Chem. Phys.* **1996**, *105*, 1142−1152. (b) Silvestrelli, P. L.; Bernasconi, M.; Parrinello, M. *Chem. Phys. Lett.* **1997**, *277*, 478−482. (c) Marx, D.; Tuckerman, M. E.; Hutter, J.; Parrinello, M. *Nature* **1999**, *397*, 601−604. (d) Geissler, P. L.; Dellago, C.; Chandler, D.; Hutter, J.; Parrinello, M. *Science* **2001**, *291*, 2121−2124. (e) Tuckerman, M. E., Marx, D.; Parrinello, M. *Nature* **2002**, *417*, 925−929. (f) Chen, B.; Ivanov, I.; Klein, M. L.; Parrinello, M. *Phys. Rev. Lett.* **2003**, *91*, 215503. See also references cited in c−f.
(75) (a) Silvestrelli, P. L.; Parrinello, M. *Phys. Rev. Lett.* **1999**, *82*, 3308−3311. (b) Silvestrelli, P. L.; Parrinello, M. *J. Chem. Phys.* **1999**, *111*, 3572−3580.
(76) (a) Gaigeot, M.-P.; Sprik, M. *J. Phys. Chem. B* **2003**, *107*, 10344−10358. (b) Gaigeot, M.-P.; Sprik, M. *J. Phys. Chem. B* **2004**, *108*, 7458−7467.
(77) Goedecker, S.; Teter, M.; Hutter, J. *Phys. Rev. B* **1996**, *54*, 1703−1710.
(78) We used CPMD, version 3.7 (IBM Corp, 1990−2003, and Max-Plank-Institut für Festkörperforshung Stuttgart, 1997−2001), developed by J. Hutter et al.
(79) Tuckerman, M. E.; Parrinello, M. *J. Chem. Phys.* **1994**, *101*, 1302−1315.
(80) Grossman, J. C.; Schwegler, E.; Draeger, E. W.; Gygi, F.; Galli, G. *J. Chem. Phys.* **2004**, *120*, 300−311.
(81) Kuo, I.-F. W.; Mundy, C. J.; McGrath, M. J.; Siepmann, J. I.; VandeVondele, J.; Sprik, M.; Hutter, J.; Chen, B.; Klein, M. L.; Mohamed, F.; Krack, M.; Parrinello, M. *J. Phys. Chem. B* **2004**, *108*, 12990−12998.
(82) Martyna, G. J.; Klein, M. L.; Tuckerman, M. E. *J. Chem. Phys.* **1992**, *97*, 2635−2643.
(83) Pagliai, M.; Raugei, S.; Cardini, G.; Schettino, V. *THEOCHEM* **2003**, *630*, 141−149.
(84) (a) Marzari, N.; Vanderbilt, D. *Phys. Rev. B* **1997**, *56*, 12847−12865. (b) Silvestrelli, P. L.; Marzari, N.; Vanderbilt, D.; Parrinello, M. *Solid State Commun.* **1998**, *107*, 7−11.
(85) Marzari, N.; Souza, I.; Vanderbilt, D. *Psi-K Newsletter* **2003**, *57*, 129−168; see http://psi-k.dl.ac.uk.
(86) Wales, D. J.; Walsh, T. R. *J. Chem. Phys.* **1996**, *105*, 6957−6971.
(87) Graf, S.; Mohr, W.; Leutwyler, S. *J. Chem. Phys.* **1999**, *110*, 7893−7908.
(88) Liu, K.; Brown, M. G.; Cruzan, J. D.; Saykally, R. J. *Science* **1996**, *271*, 62−64. (b) Liu, K.; Brown, M. G.; Cruzan, J. D.; Saykally, R. J. *J. Phys. Chem. A* **1997**, *101*, 9011−9021.
(89) Keutsch, F. N.; Saykally, R. J. *Proc. Natl. Acad. Sci. U.S.A.* **2001**, *98*, 10533−10540.
(90) Lightstone, F. C.; Schwegler, E.; Hood, R. Q.; Gygi, F.; Galli, G. *Chem. Phys. Lett.* **2001**, 343, 549−555.
(91) Bakó, I.; Hutter, J.; Pálinkás, G. *J. Chem. Phys.* **2002**, *117*, 9838−9843.
(92) (a) Laaksonen, L. *J. Mol. Graphics* 1992, *10*, 33−34. (b) Bergman, D. L.; Laaksonen, L.; Laaksonen, A. *J. Mol. Graphics Modell.* **1997**, *15*, 301−306; see also http://www.csc.fi/gopenmol.
(93) VondeVonde, J.; Mohamed, F.; Krack, M.; Hutter, J.; Sprik, M.; Parrinello, M. *J. Chem. Phys.* **2005**, *122*, 014515.